Original Research Article

Early weaning leads to the remodeling of lipid profile in piglet jejunal crypt cells during post-weaning days

Yirui Shao [a, b], Xia Xiong [a, *], Kexing Wang [c], Pi Cheng [d], Lijun Zou [e], Jian Zhou [a, b], Ming Qi [a, b], Yulong Yin [a]

[a] CAS Key Laboratory of Agro-ecological Processes in Subtropical Region, Institute of Subtropical Agriculture, Hunan Province Key Laboratory of Animal Nutritional Physiology and Metabolic Process, National Engineering Laboratory for Pollution Control and Waste Utilization in Livestock and Poultry Production, Institute of Subtropical Agriculture, Chinese Academy of Sciences, Changsha 410125, China
[b] University of Chinese Academy of Sciences, Beijing 100008, China
[c] Laboratory of Animal Nutrition and Human Health, College of Life Sciences, Hunan Normal University, Changsha 410081, China
[d] Hunan Key Laboratory of Traditional Chinese Veterinary Medicine, Hunan Agricultural University, Changsha 410128, China
[e] Laboratory of Basic Biology, Hunan First Normal University, Changsha 410205, China

ARTICLE INFO

ABSTRACT

Reportedly, proteins involved in lipid metabolism change significantly in the jejunal crypt cells of early-weaned piglets, but the exact lipid profile change remains uncertain. In the present study, 32 piglets weaned at 21 d of age were randomly divided into 4 groups with 8 replicates. The jejunal crypt cells of a group of piglets on the post-weaning day (PWD) 1, 3, 7, and 14 were isolated per time point. Crypt cell lipid profiles were analyzed using ultra-high-performance liquid chromatography coupled with hybrid quadrupole time-of-flight mass spectrometry. This study showed that piglets suffered the greatest weaning stress on PWD 3 in terms of the lowest relative weight of the small intestine, the highest relative weight of the spleen, and the highest levels of malondialdehyde, cholesterol, and low-density lipoprotein cholesterol. The lipid profile of jejunal crypt cells including carnitine, sulfatide, sphingomyelin, hexosylceramide, and ceramide greatly changed after weaning, especially between PWD 3 and 14 ($P < 0.05$). The differential lipid species between these 2 d were mainly involved in the glycerophospholipid metabolism pathway. In addition, potential lipid biomarkers for weaning stress in crypt cells such as phosphatidylcholine (PC) (9:0/26:1), PC (17:0/18:2), carnitine (24:0), carnitine (22:0), sphingomyelin (d14:1/22:0), PC (P-18:0/18:4), phosphatidylethanolamine (P-16:0/20:4), phosphatidylinositol (15:1/24:4), and dihexosylceramide (d14:1/26:1) were identified. The changes in lipid profile might be related to the inflammation caused by early weaning. These findings might provide new therapeutic targets for intestinal dysfunctions caused by weaning stress.

© 2022 The Authors. Publishing services by Elsevier B.V. on behalf of KeAi Communications Co. Ltd. This is an open access article under the CC BY-NC-ND license (http://creativecommons.org/licenses/by-nc-nd/4.0/).

1. Introduction

Early weaning is a universally technique used for enhancing pork production. The weaning ages shift from 5 to 7 weeks to 3 to 4 weeks (Widowski et al., 2008). However, maternal deprivation, dietary changes, transportation, and social stress may contribute to weaning stress (Latham and Mason 2008; Campbell et al., 2013). Weaning stress further leads to declined feed intake, diarrhea, intestinal barrier impairment, and disorganized gut microbiota, causing economic losses in the pig industry (Dong and Pluske 2007; Lecce 1986; Smith et al., 2010; Castillo et al., 2007).

The jejunum is the principal part of the small intestine involved in nutrient absorption, such as fat, carbohydrate, and protein (Suzuki et al., 2009). Jejunal epithelium undergoes rapid self-renewing processes, in which proliferation, differentiation, apoptosis, and cell shedding are concisely regulated along the

crypt—villus axis (Gordon and Hermiston 1994). The continuous proliferation and differentiation of intestinal crypt cells lead to epithelial renewal and the repair of injuries (van der Flier and Clevers 2009). As the major components of biomembranes, phospholipids and cholesterols are indispensable for cell division (Ito and Suda 2014; Wang et al., 2018a). They also serve as energy-storage molecules and regulators for signal transduction, cytoskeletal regulation, and membrane trafficking (Walther and Farese 2012; Martin 1998). Weaning stress leads to deeper crypt depth, and proteins involved in lipid and fatty acid metabolism change remarkably in the jejunal crypt cells of early-weaned piglets, according to our previous study (Yang et al., 2016; van Beers-Schreurs et al., 1998). However, the effect of early weaning on changes in the lipid profile in jejunal crypt cells remains unknown. Therefore, the present study focused on the effect of weaning stress on the dynamic changes of lipid profile in piglet jejunal crypt cells during post-weaning days (PWD). This study might provide a new perspective for understanding the effect of weaning stress on the intestine and aid in the development of new therapies.

2. Materials and methods

2.1. Animal ethics

The experimental procedure was conducted following the guidelines of the Animal Care and Use Committee of the Institute of Subtropical Agriculture, Chinese Academy of Sciences (2013020).

2.2. Animals and diets

As reported in our previous study (Zhou et al., 2019), a total of 32 piglets (Landrace × Yorkshire × Duroc) with similar weight (7.55 ± 0.16 kg) were weaned at 21 d of age (half of the piglets were female). Piglets were randomly divided into 4 groups ($n = 8$) and housed individually in pens with a hard-plastic slatted floor under identical environmental conditions. All piglets were fed the same basal diet that met the nutrient requirements recommended in 2012 by the National Research Council (NRC, 2012). Furthermore, all animals had free access to food and water throughout the experimental period.

2.3. Sampling

On PWD 1, 3, 7, and 14, a group of piglets per time point were weighed. As reported in our previous study (Zhou et al., 2019), the mean weights of the piglets were 7.28 ± 0.31, 7.39 ± 0.31, 8.84 ± 0.42, and 9.78 ± 0.55 kg (mean ± SEM) accordingly. They were sacrificed with an intravenous (jugular vein) injection of 4% sodium pentobarbital solution (40 mg/kg body weight; Sigma, St. Louis, MO, USA) (Yang et al., 2016). Blood samples were collected in 10-mL tubes before individuals were sacrificed and centrifuged at 3,000 × g at 4 °C for 10 min to be used for further analysis (Yang et al., 2013b). The stomach, small intestine, and large intestine were removed and weighed after being gently rinsed with a 0.9% NaCl solution and having mesenteries and fat removed. The spleen was then removed and weighed.

2.4. Isolation of jejunal crypt cells

Piglet jejunal crypt cells were isolated as described in our previous study (Xiong et al., 2015). In short, mid-jejunum was separated into segments, thoroughly rinsed with ice-cold physiological saline solution, and incubated with oxygenated phosphate buffer saline at 37 °C for 30 min. These segments were then incubated with 200 mL of oxygenated chelating buffer (5 mM Na₂EDTA, 10 mM HEPES with pH 7.4, 0.5 mM dithiothreitol [DTT], 0.25% bovine serum albumin [BSA], 2.5 mM D-glucose, 2.5 mM L-glutamine, 0.5 mM dl-β-hydroxybutyrate sodium salt; oxygenated with an O₂/CO₂ mixture [19:1, vol/vol], pH 7.4) at 37 °C for 40 min and then centrifuged at 400 × g for 10 min at 4 °C to obtain the supernatant. The crypt fraction was harvested after repeating this procedure 3 times. The crypt fraction was washed twice with the oxygenated cell resuspension buffer (10 mM HEPES, 1.5 mM CaCl₂, 2.0 mM MgCl₂; pH 7.4) and then centrifuged at 400 × g at 4 °C for 4 min. The supernatant was discarded, and the cell pellet was immediately frozen in the liquid nitrogen and then stored at −80 °C.

2.5. Organ indexes and serum biochemical indexes

The organ indexes of the stomach, small intestine, large intestine, and spleen were calculated as the percentage of body weight. Four biochemical parameters, including high-density lipoprotein cholesterol (HDL-C), low-density lipoprotein cholesterol (LDL-C), triglyceride (TG), and cholesterol (CHOL), were measured in the serum samples using a biochemical analyzer (TBA-120FR, Toshiba Medical Systems Corporation, Tokyo, Japan). Lipid peroxidation was evaluated by measuring the malondialdehyde (MDA) level using the MDA detecting kit (Nanjing Jiancheng Bioengineering Institute) following the manufacturer's instructions.

2.6. Real-time quantitative polymerase chain reaction (RT-qPCR)

RNA was extracted, and RT-qPCR was performed following our previous study (Qi et al., 2020). Briefly, total RNA was isolated from the cell pellet using TRIZOL reagent (Invitrogen, Carlsbad, CA, USA). The concentration and quality of the RNA were determined by the NanoDrop ND-2000 Spectrophotometer (Thermo Fisher Scientific, Waltham, MA, USA) and the 1% agarose electrophoresis. Complementary DNA (cDNA) was synthesized using the PrimeScript RT reagent kit with gDNA Eraser (Takara Biotechnology Co., Ltd., Dalian, China) following the manufacturer's instructions. The RT-qPCR for genes was performed in triplicates using the SYBR Green Premix Pro Taq HS qPCR Kit (Accurate Biotechnology [Hunan] Co., Ltd.) on a LightCycler480 Real-Time PCR system (Roche Diagnostics, Germany). The sequences of primers and references are listed in Table 1. The relative gene expression was normalized by β-actin using the $2^{-\Delta\Delta Ct}$ method (Livak and Schmittgen 2001). Data were expressed as the relative values to those on PWD 1.

2.7. Metabolite extraction

Liquid chromatography—mass spectrometry (LC—MS) grade methanol and methyl *tert*-butyl ether (MTBE) were purchased from CNW Technologies (Düsseldorf, Germany). LC—MS grade ammonium acetate, ammonium hydroxide, dichloromethane (DCM), and isopropyl alcohol (IPA) were purchased from Merk & Co (Kenilworth, NJ, USA).

Fifty milligrams of the sample were put into an Eppendorf tube, and 200 μL water and 480 μL extraction liquid ($V_{MTBE}:V_{MeOH} = 5:1$) were added. After being homogenized in a ball mill for 4 min at 45 Hz, the tube was treated with ultrasound for 5 min (ice water bath). After being homogenized 3 times, the tube was incubated at −20 °C for 1 h to precipitate proteins. The tube was then centrifuged at 16,312 × g at 4 °C for 15 min. The supernatant (380 μL) was transferred into a new Eppendorf tube and dried in a vacuum concentrator without heating. The dried extract was then reconstituted in 100 μL extraction solution ($V_{DCM}:V_{MeOH} = 1:1$), vortexed for 30 s, sonicated for 10 min (incubated in 4 °C water), and centrifuged (13,899 × g, 15 min, 4 °C). Sixty microliters of the supernatant were transferred into a fresh 2 mL LC/MS glass vial for the ultra-high performance liquid chromatography (UHPLC)

Table 1
Primer pairs used for the real-time quantitative polymerase chain reaction.

Gene	GenBank no.	Sequence (5′ to 3′)	Product length, bp	Reference
β-actin	XM_003124280.5	F: CTGCGGCATCCACGAAACT	147	Yin et al. (2018)
		R: AGGGCCGTGATCTCCTTCTG		
IL-1β	NM_214055.1	F: ACGTGCAATGATGACTTTGTCTG	113	Ren et al. (2021)
		R: AGAGCCTTCAGCATGTGTGG		
IL-8	NM_213867.1	F: TAGGACCAGAGCCAGGAAGA	92	Su et al. (2021)
		R: AGCAGGAAAACTGCCAAGAA		
TNF-α	NM_214022.1	F: CATCGCCGTCTCCTACCA	199	Wang et al. (2019)
		R: CCCAGATTCAGCAAAGTCCA		

IL-8 = interleukin-8; IL-1β = interleukin-1β; TNF-α = tumor necrosis factor-α.

coupled with hybrid quadrupole time-of-flight mass spectrometry (QTOF-MS) analysis. Blank and quality control (QC) samples were used to make sure the analysis results were reliable.

2.8. LC−MS/MS analysis

The UHPLC system (1290, Agilent Technologies) was used to perform LC−MS/MS analyses using a Phenomen Kinetex C18 100A Column (100 × 2.1 mm, 1.7 μm) coupled with a Triple TOF 5600 (Q-TOF, AB Sciex) mass spectrometer. The mobile phase (A: 10 mM $HCOONH_4$ + 40% H_2O + 60% acetonitrile [ACN], B: 10 mM $HCOONH_4$ + 10% ACN + 90% IPA) was carried with an elution gradient (0 min, 40% B; 12 min,100% B; 13.5 min, 100% B; 13.7 min, 40% B; 18 min, 40% B), which was delivered at 300 μL/min. A triple TOF mass spectrometer (5600, AB Sciex), controlled by the acquisition software (Analyst TF 1.7, AB Sciex), was used to acquire tandem mass spectrometry (MS/MS) spectra based on the information-dependent basis (IDA). The ESI source parameters were set as follows: GS1: 60 psi; GS2: 60 psi; CUR: 30 psi; source temperature 550 °C; ion spray voltage floating (ISVF) field, 5,500 V (positive mode) or −4,500 V (negative modes).

2.9. Data processing and annotation

MS raw data were converted to the mzXML format using Proteo-Wizard and further analyzed using the R package XCMS (version 3.2). The minfrac was set as 0.5, and the cutoff was set as 0.6. R package CAMERA (version 1.40.0) and the in-house MS2 database were used for peak annotation and metabolites identification, respectively. Lipidomics data from positive and negative modes were combined for further analysis. If a lipid species was detected in both modes, the one with a higher MS2 score was conserved. Data were then de-noised, and the missing values were filled by half of the minimum value.

Further, the data were processed by total ion current normalization and then run through SIMCA (version 4.1, Sartorius Stedim Data Analytics AB, Umea, Sweden) for principal component analysis (PCA) and orthogonal projections to latent structures-discriminate analysis (OPLS-DA). The pathways of lipids were analyzed using the Kyoto Encyclopedia of Genes and Genomes (KEGG) (https://www.genome.jp/kegg/) and MetaboAnalyst 4.0 (https://www.metaboanalyst.ca/). To identify lipid biomarkers for weaning stress, we identified lipids showing the same change pattern as MDA using PatternHunter in MetaboAnalyst 4.0, based on Spearman's distance measure.

2.10. Correlation analysis

The 9 lipid species with the highest absolute values of Spearman's correlation coefficient were selected, and correlations between their relative abundance and serum biochemical index levels were evaluated. Correlation analysis was performed using Spearman's correlation analysis, and diagrams were created using R (version 4.0.2).

2.11. Statistical analysis

Data are presented as means ± SEM, and $P < 0.05$ was considered statistically significant. The significance of differences was determined using one-way analysis of variance (ANOVA) with post−hoc comparisons made by the least significant difference (LSD) test (for normally distributed data with equal variance) or using Kruskal−Wallis ANOVA and a Dunn−Bonferroni test for post hoc comparisons (for non-normal distributed or data with unequal variance). The variable importance in the projection (VIP) was obtained from OPLS-DA analysis, and differences between the 2 groups were accessed by Student's t-test. Lipids species (VIP > 1 and $P < 0.05$) were defined as differential lipid species. Metabolic pathways with impact values of more than 0.10 were identified as potential pathways affected by weaning stress (Wang et al., 2018b). Data analysis and figures were performed using IBM SPSS Statistics (version 22.0; SPSS Inc., Chicago, USA), OriginPro 9.4 (OriginLab Corporation, Northampton, USA), and GraphPad Prism 8.0.2 (GraphPad Software, San Diego, CA, USA).

3. Results

3.1. Effect of weaning stress on organ indexes

The relative weights of the stomach on PWD 3, 7, and 14 were significantly higher than that on PWD 1 ($P < 0.05$; Table 2). The

Table 2
Organ indexes of piglets on different PWD (weaned at 21 d of age).[1]

Item	Groups			
	PWD 1	PWD 3	PWD 7	PWD 14
Stomach, g/kg	5.07 ± 0.17[b]	6.40 ± 0.31[a]	6.47 ± 0.33[a]	6.72 ± 0.34[a]
Small intestine, g/kg	34.41 ± 1.68[a]	27.06 ± 1.09[b]	36.77 ± 0.91[a]	37.70 ± 1.62[a]
Large intestine, g/kg	6.53 ± 1.66[b]	8.96 ± 0.50[b]	14.48 ± 0.80[a]	12.92 ± 0.60[a]
Spleen, g/kg	2.32 ± 0.21[b]	3.04 ± 0.13[a]	2.41 ± 0.21[ab]	2.30 ± 0.10[b]

PWD = post-weaning days.
[a,b]Values in the same row with different superscripts are significantly different ($P < 0.05$).
[1] Values are expressed as means ± SEM ($n = 8$).

relative weight of the small intestine on PWD 3 was significantly lower than that on PWD 1, 7, and 14 ($P < 0.05$). Furthermore, the relative weight of the spleen on PWD 3 was significantly higher than that on PWD 1 and 14 ($P < 0.05$).

3.2. Effect of weaning stress on serum biochemical indexes

The serum MDA level was the highest on PWD 3 and the lowest on PWD 14. Its level on PWD 1 and 3 was significantly higher than on PWD 14 ($P < 0.05$; Fig. 1A). The serum CHOL, HDL-C, and LDL-C levels were significantly decreased on PWD 7 and 14 compared to PWD 1 and 3 ($P < 0.05$; Fig. 1B).

3.3. Effect of weaning stress on pro-inflammatory cytokine mRNA expression in jejunal crypt cells

The mRNA expression of tumor necrosis factor-α (TNF-α) on PWD 7 and 14 was significantly lower than PWD 1 and 3 ($P < 0.05$; Fig. 2A).

3.4. Effect of weaning stress on lipid composition of the jejunal crypt cells

There were 973 lipid species successfully identified in the negative and positive ion mode (Fig. 3B), including phosphatidylcholine (PC; 230, 23.6%), phosphatidylethanolamine (PE, 199, 20.5%), triacylglycerol (TAG; 119, 12.2%), phosphatidylglycerol (PG; 100, 10.3%), ceramide (Cer; 66, 6.8%), phosphatidylinositol (PI; 66, 6.8%), phosphatidic acid (PA; 53, 5.4%), and others (140, 14.4%) including sulfatide, phosphatidylserine, carnitine, cholesteryl ester, ceramide-1-phosphate, diacylglycerol (DG), monoacylglycerol, hexosylceramide (HexCer), dihexosylceramide (Hex2Cer), sphingomyelin (SM), and sphingosine.

Unsupervised PCA revealed noticeable separations among all PWD (except between PWD 7 and 14) in crypt cells (Fig. 3A). The lipid species of PC, PE, and TAG in crypt cells were predominant during different PWD (Fig. 3C to F). Furthermore, the relative abundance of lipid classes in each group was compared. The relative abundance of HexCer, Hex2Cer, sulfatide, SM, and carnitine in jejunal crypt cells on PWD 3 was significantly higher ($P < 0.05$), and the relative abundance of Cer and DG on PWD 3 was significantly lower ($P < 0.05$) than those on PWD 7 and 14 (Fig. 4B, C, D). Moreover, the relative abundance of PC was significantly lower ($P < 0.05$) on the PWD 3 than that on PWD 14 (Fig. 4A), and the PC/PE ratio on PWD 3 was the lowest among all the PWD (Fig. 4E).

3.5. Lipid metabolic pathway differences between PWD 3 and 14

Differential lipid species ($P < 0.05$, VIP > 1) between PWD 3 and 14 in crypt cells (Supplementary Table S1) were analyzed with MetaboAnalyst 4.0. As shown in Table 3 and Fig. 5, differential lipid species were enriched in 5 metabolic pathways in crypt cells. Pathways with an impact value greater than 0.10 were defined as potential pathways affected by weaning stress (Wang et al., 2018b). Glycerophospholipid metabolism was significantly enriched (raw $P < 0.01$) with an impact value of 0.199. Differential lipid species involved in glycerophospholipid metabolism were mainly composed of PE and PC (Supplementary Table S2).

3.6. Lipid biomarker analysis for weaning stress on intestinal crypt cells

Lipid species with the similar change mode as MDA during PWD (the level was relatively higher or lower on PWD 1 and 3, and gradually decreased or increased, respectively, till PWD 14) were identified (Fig. 6A). The top 9 lipid species were selected
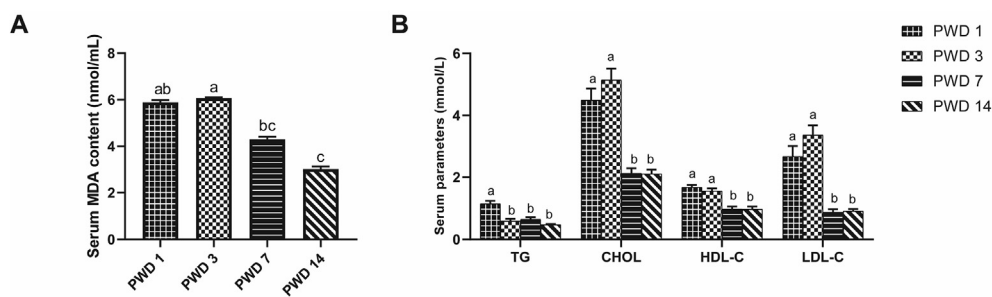

Fig. 1. The malondialdehyde (MDA) level and serum biochemical indexes of piglets weaned at 21 d of age on different post-weaning days (PWD). (A) Serum MDA level of weaned piglets. (B) Serum biochemical indexes of weaned piglets. [abc]Values with different letters are significantly different ($P < 0.05$). Data are presented as means ± SEM ($n = 8$). HDL-C = high-density lipoprotein cholesterol; LDL-C = low-density lipoprotein cholesterol; TG = triglyceride; CHOL = cholesterol.
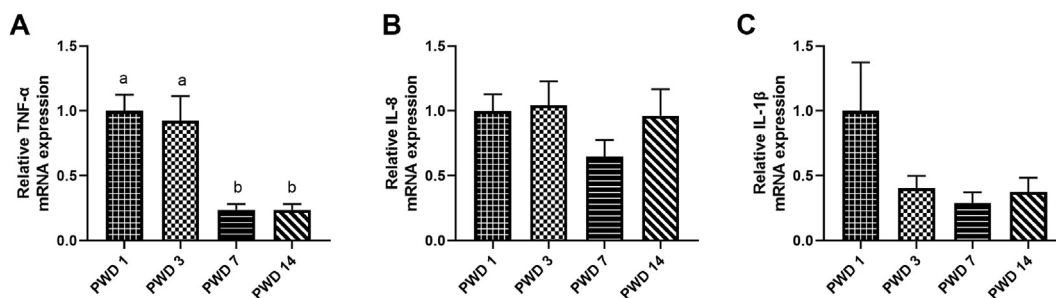

Fig. 2. Relative mRNA expression of pro-inflammatory cytokine in piglet jejunal crypt cells on different PWD (weaned at 21 d of age). (A to C) Relative mRNA expression of TNF-α, IL-8, and IL-1β in jejunal crypt cells. [a,b]Values with different letters are significantly different ($P < 0.05$). Data are presented as means ± SEM ($n = 8$). PWD = post-weaning days; IL-8 = interleukin-8; IL-1β = interleukin-1β; TNF-α = tumor necrosis factor-α.
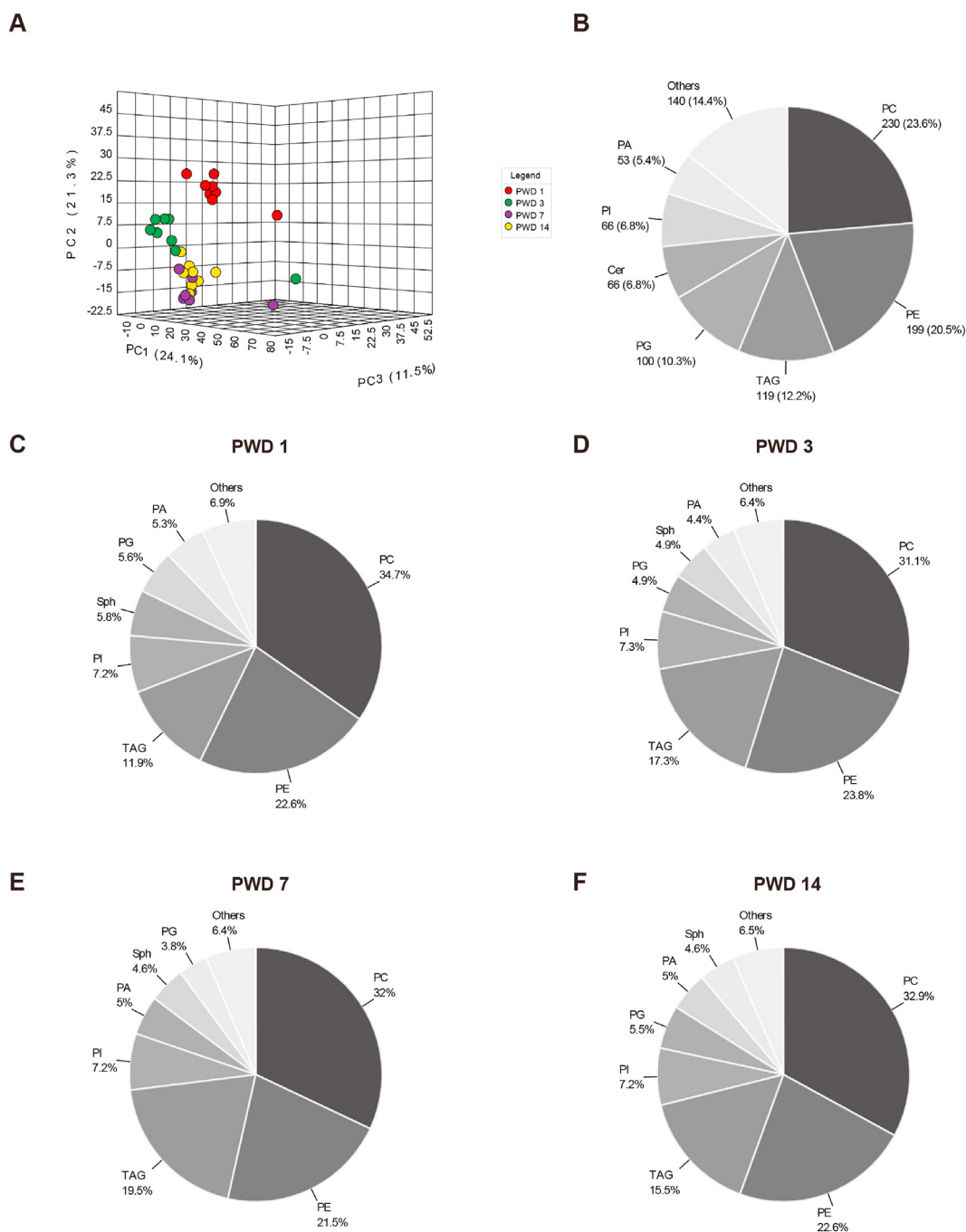
Fig. 3. Lipidomic analysis of piglet jejunal crypt cells on different PWD (weaned at 21 d of age, $n = 8$). (A) Principal component analysis score plots of the metabolic profile of intestinal crypt cells. (B) The distribution of identified lipid species in the intestinal crypt cells. (C to F) The percentage of lipids in the total identified lipid species on PWD 1, 3, 7, and 14. PWD = post-weaning days; Cer = ceramide; PA = phosphatidic acid; PG = phosphatidylglycerol; PI = phosphatidylinositol; TAG = triacylglycerol; PC = phosphatidylcholine; PE = phosphatidylethanolamine; Sph = sphingosine.

based on the correlation coefficients. The levels of PC (P-18:0/18:4), PI (15:1/24:4), SM (d14:1/22:0), Hex2Cer (d14:1/26:1), carnitine (22:0), carnitine (24:0), and PE (P-16:0/20:4) were continuously decreased, the levels of PC (17:0/18:2) and PC (9:0/26:1) were continuously increased in crypt cells during PWD (Fig. 6C).

A correlation analysis between the relative abundance of the lipid markers and the levels of MDA, TG, HDL-C, CHOL, and LDL-C in the serum as well as the *IL-8*, *IL-1β*, and *TNF-α* mRNA expression in jejunal crypt cells was performed. The present study showed that

most markers significantly correlated with the concentrations of MDA, TG, HDL-C, CHOL, LDL-C, and *TNF-α* mRNA levels (Fig. 6B).

4. Discussion

Early weaning is one of the most stressful events for piglets in the pig farming industry, as they undergo structural and functional changes in the intestine (Campbell et al., 2013). Crypt cells play a critical role in supporting homeostasis, regeneration, and repairment of intestinal epithelial cells (Andersson-Rolf et al., 2017;
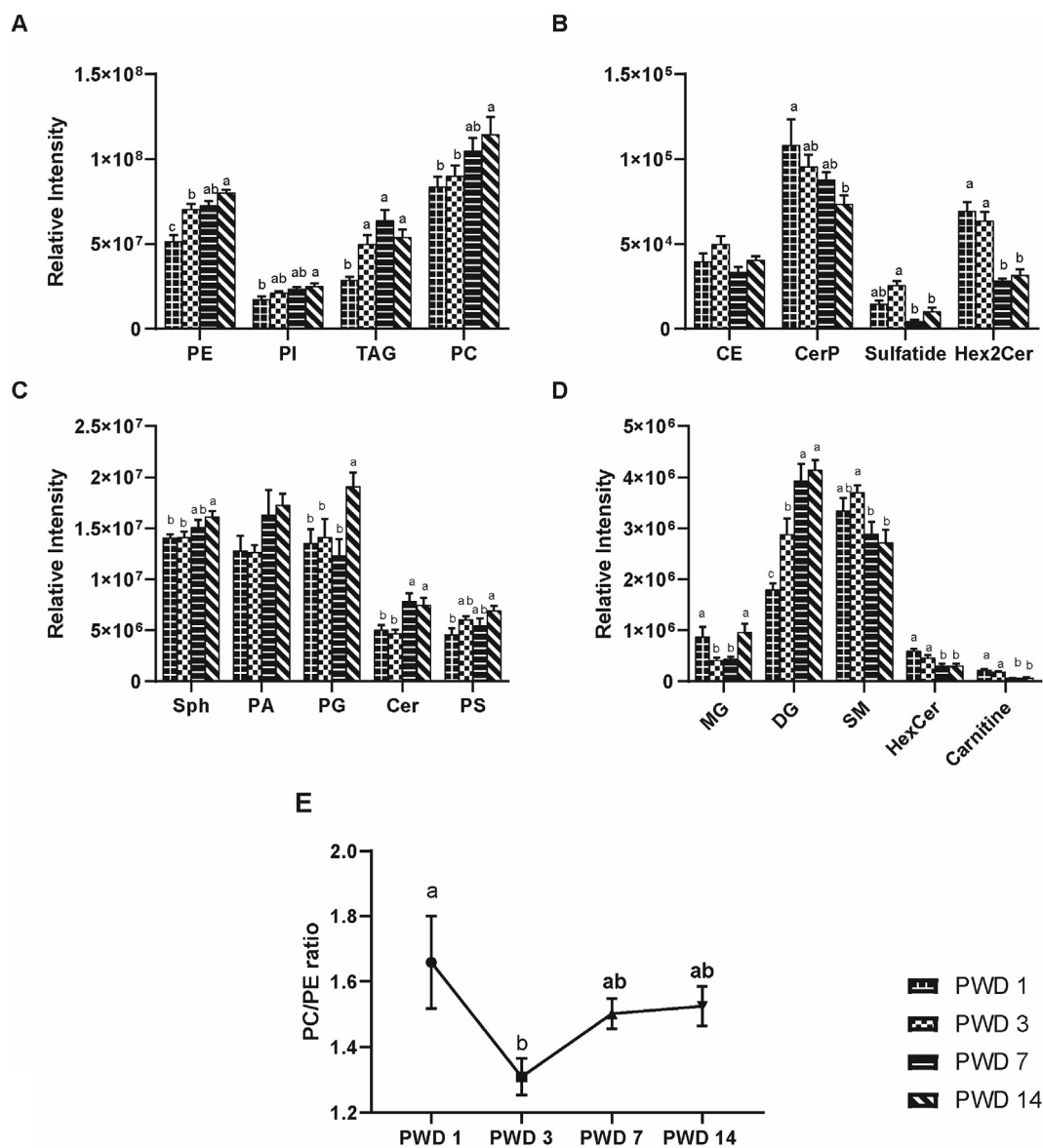
Fig. 4. Lipid classes analysis of piglet jejunal crypt cells on different PWD (weaned at 21 d of age). (A to D) Relative mass spectrometry intensity of lipid classes of piglet intestinal crypt cells. (E) PC/PE ratio of intestinal crypt cells. [a,b,c]Values with different lowercase letters are significantly different ($P < 0.05$). Data are presented as means ± SEM ($n = 8$). PWD = post-weaning days; CE = cholesteryl ester; Cer = ceramide; CerP = ceramide-1-phosphate; DG = diacylglycerol; MG = monoacylglycerol; PA = phosphatidic acid; PG = phosphatidylglycerol; PI = phosphatidylinositol; PS = phosphatidylserine; HexCer = hexosylceramide; Hex2Cer = dihexosylceramide; SM = sphingomyelin; PC = phosphatidylcholine; PE = phosphatidylethanolamine; Sph = sphingosine; TAG = triacylglycerol.

Table 3
Metabolic pathways involved in lipid species with significantly different levels[1] between PWD 3 and 14 in piglet jejunal crypt cells.

Metabolic pathways	Total	Hits[2]	Raw P-value	−log (P-value)	Holm P-value[3]	Impact
Glycerophospholipid metabolism	36	2	0.002	2.809	0.130	0.199
Linoleic acid metabolism	5	1	0.010	2.015	0.801	0.000
Alpha-linolenic acid metabolism	13	1	0.025	1.603	1.000	0.000
Glycosylphosphatidylinositol-anchor biosynthesis	14	1	0.027	1.571	1.000	0.004
Arachidonic acid metabolism	36	1	0.068	1.167	1.000	0.000
Glycerophospholipid metabolism	36	2	0.002	2.809	0.130	0.199

PWD = post-weaning days.
[1] Lipid species with significantly different levels: $P < 0.05$ and variable importance in the projection > 1.
[2] Hit: the matched number of metabolites in the pathway.
[3] Holm P-value: adjusted P-value with the Holm−Bonferroni method.

Barker 2014). As shown in the present study, weaning affected organ indexes, serum biochemical indexes, jejunal crypt mRNA expression, and lipid profile of piglets, especially between PWD 3 and 14. Our study revealed the dynamic lipid changes in piglet jejunal crypt cells after weaning, in which post-weaning inflammation might play an important role.
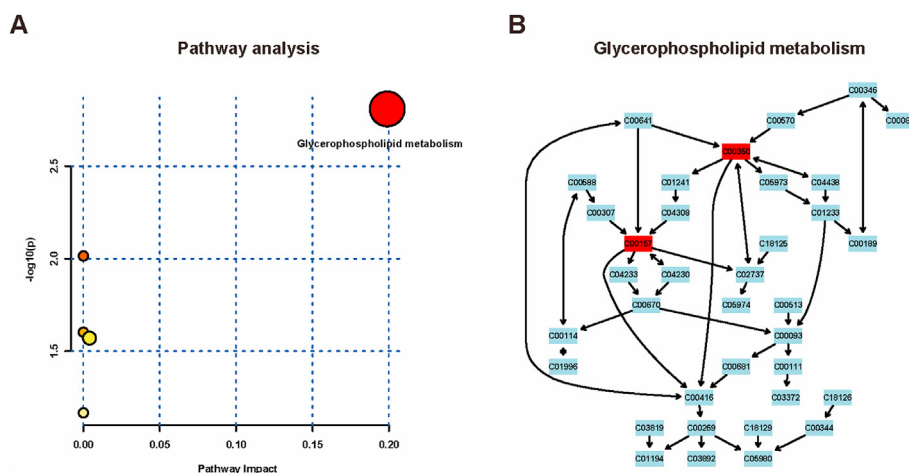
Fig. 5. Pathways analysis of differentially expressed lipid species in piglet jejunal crypt cells between post-weaning days 3 and 14 (weaned at 21 d of age). (A) Summary of the metabolic pathways involved in lipid species with significantly different levels ($P < 0.05$ and variable importance in the projection >1). Color gradient represents the significance of the pathway ranked by P-value (yellow, higher P-value; red, lower P-value). Circle size indicates the pathway impact score (a larger circle represents a higher impact score). Pathways with impact scores higher than 0.10 are identified by name. Labels within small boxes correspond to KEGG identifiers for metabolites. (B) Pathway of glycerophospholipid metabolism. Phosphatidylcholine (C00157) and phosphatidylethanolamine (C00350) are hit and colored in red in the boxes.

Serum MDA, CHOL, HDL-C, and LDL-C levels were determined to assess changes in lipid metabolism of weaned piglets. Our results showed that the content of MDA, the lipid peroxidation product, peaked on PWD 3 and reached the bottom on PWD 14, which corresponded to the result of our previous study (Yin et al., 2014). Reportedly, inflammation and oxidative stress could lead to an enlarged spleen (Cho et al., 2011; Khan et al., 1999). In the present study, the relatively heavier spleen and lighter small intestine on PWD 3 revealed that weaning stress inhibited small intestine growth and contributed to splenic enlargement on PWD 3. Further, the highest CHOL and LDL-C levels in the serum implied a severe lipid metabolism disorder on PWD 3. Collectively, the early-weaned piglets might suffer the greatest oxidative damage on PWD 3 and gradually restored on PWD 14.

Intestinal epithelial cells are renewed rapidly (about every 3 to 5 d). Crypt cells play a critical role in replenishing lost cells, contributing to the renewal and damage repairment of the intestinal epithelium (Yang et al., 2013a). As the primary component of cells, lipids play a crucial role in animal development and immunity (Hubler and Kennedy 2016; Palm and Rodenfels 2020). By examining the jejunal crypt lipidome of early-weaned piglets, we have broadened the understanding of lipid changes during PWD. According to the lipidome, most of the identified lipid species were PE and PC, the most abundant phospholipids in the mammalian cellular membrane (van der Veen et al., 2017). In the current study, lipid classes with different levels among PWD were mainly phospholipids or sphingolipids. Within the last decade, it has become evident that sphingolipids are critical regulators in cell renewal, metabolism, and immunity (Espaillat et al., 2017). Reportedly, SM and Cer act as regulators of immune cells in alleviating colitis, and dextran sodium sulfate treatment leads to a noticeable decrease of SM in Caco-2 cells (Li et al., 2020; Espaillat et al., 2017). Notably, the jejunal crypt *TNF-α* mRNA level remarkably increased on PWD 3 in this study, which was consistent with the fact that weaning contributes to intestinal inflammation in piglets (Li et al., 2021; Meng et al., 2019). Thus, the increased inflammation level in jejunal crypt cells on PWD 3 might be partly due to the downregulated Cer level. However, the SM level unexpectedly elevated on PWD 3 in this study. According to the KEGG database, SM can be transformed into Cer by sphingomyelin phosphodiesterase 1, and Cer can be transformed into SM by sphingomyelin synthase 1. Therefore, the

increased level of SM on PWD 3 might be due to the compromised synthesis of SM from Cer.

It has been reported that PC treatment ameliorates acetic acid-induced colitis in rats, and the decreased PC level in the intestinal mucus layer is related to ulcerative colitis (Braun et al., 2009; Fabia et al., 1992). Moreover, decreased PC/PE ratio implies impaired cellular membrane integrity (Li et al., 2006). Hence, we speculate that the decreased PC level and PC/PE ratio on PWD 3 in this study might be relevant to the inflammation in crypt cells of early-weaned piglets. Further, the increased relative abundance of sulfatide on PWD 3 in our results is consistent with the fact that sulfatide produced from sites of inflammation can further intensify the inflammatory reaction by regulating immune cells (Jeon et al., 2008; Constantin et al., 1994). As a widely used antioxidant, L-carnitine pretreatment has been reported to slow bacterial translocation, secretion of pro-inflammatory cytokines, and intestinal mucosal injury during ischemia/reperfusion in rats (Yuan et al., 2011). Furthermore, L-carnitine pretreatment could also alleviate mitochondrial dysfunction and DNA injury, lipid peroxidation, and apoptosis of epithelial cells induced by cisplatin in the small intestine of rats (Chang et al., 2002). However, the relative abundance of carnitine remarkably increased on PWD 3 in this study. The increased carnitine might implicate the self-defense of piglets against the weaning stress, but the underlying mechanism needs further exploration. Taken together, early weaning disturbed lipid profile in crypt cells, especially on PWD 3, and these changes might be related to inflammation caused by weaning stress.

As the difference in MDA level between PWD 3 and 14 was the greatest, we focused on the differences in lipid composition between PWD 3 and 14 in the following analysis. Differential lipid species between PWD 3 and 14 were involved in glycerophospholipid metabolism. Glycerophospholipids are components of biomembranes, bile, and membrane surfactants. A previous study reported that the glycerophospholipid level increased remarkably under inflammation (Yang et al., 2019). Similarly, glycerophospholipid metabolism has been proven to be relevant to non-alcoholic fatty pancreas disease and type 2 diabetes mellitus, in which PE and PC play a key role (Lin et al., 2019). Therefore, our findings suggested that early weaning influenced glycerophospholipid metabolism, consequently leading to specific lipid changes, such as PE and PC, which might participate in the
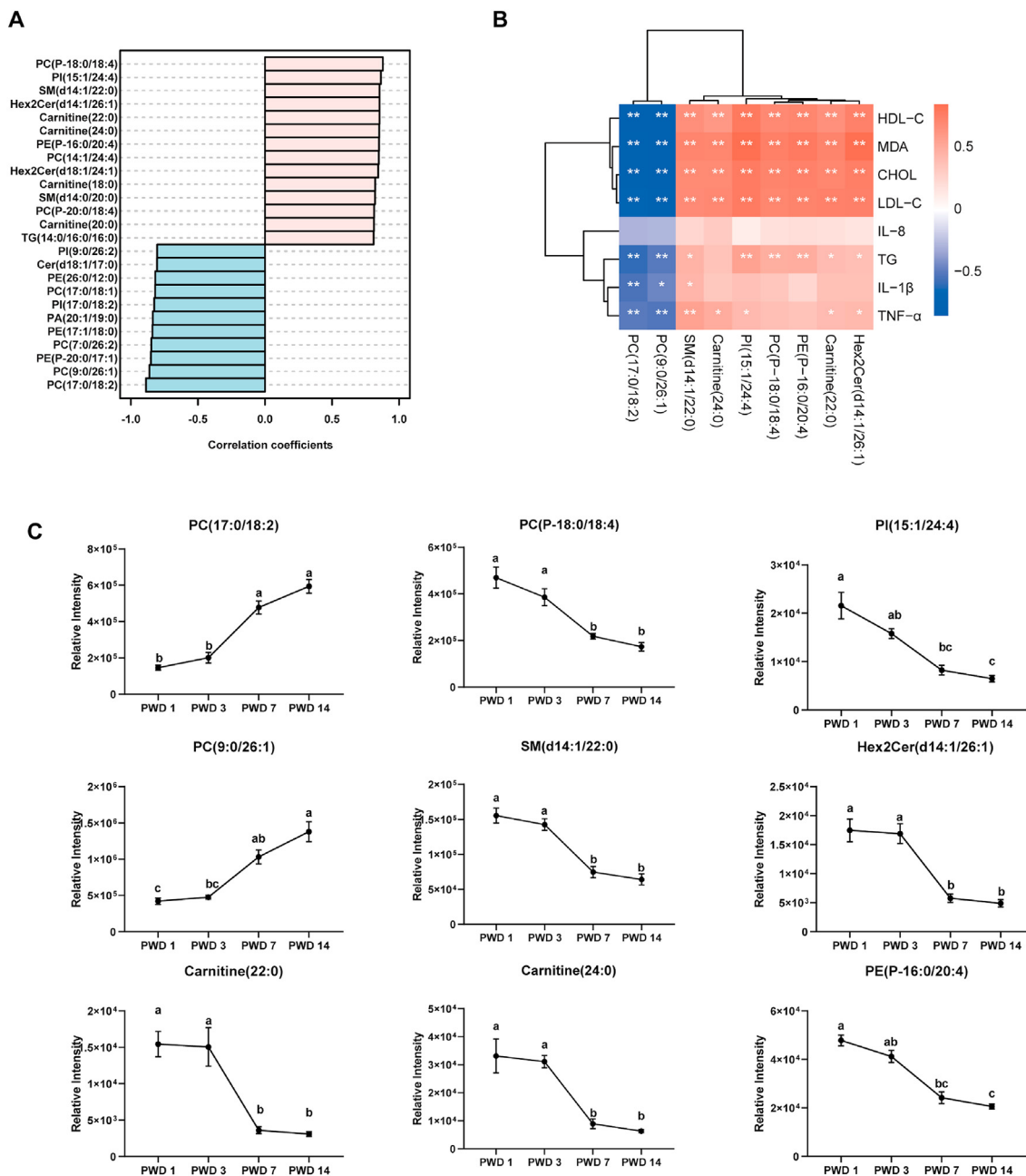
Fig. 6. Lipid biomarker analysis for weaning stress. (A) Top 25 lipid biomarkers with the "3—3—2—1" pattern based on Spearman's correlation analysis. (B) Correlation analysis of the top 9 lipid species abundances and serum biochemical index levels based on Spearman's correlation analysis. *P < 0.05, **P < 0.01. (C) Changes in the relative abundance of the top 9 lipid markers during the post-weaning day. ^{abc}Values with different lowercase letters are significantly different (P < 0.05). Data are presented as means ± SEM (n = 8). PWD = post-weaning days; MDA = malondialdehyde; HDL-C = high-density lipoprotein cholesterol; LDL-C = low-density lipoprotein cholesterol; TG = triglyceride; CHOL = cholesterol; Cer = ceramide; PA = phosphatidic acid; PI = phosphatidylinositol; Hex2Cer = dihexosylceramide; SM = sphingomyelin; PC = phosphatidylcholine; PE = phosphatidylethanolamine; TAG = triacylglycerol; *IL-8* = interleukin-8; *IL-1β* = interleukin-1β; *TNF-α* = tumor necrosis factor-α.

inflammation of jejunal crypt cells after weaning. However, most pathway analysis tools can only illustrate lipid classes (Wang and Zhu 2021); analysis of pathways involved in different lipid species remains to be further elucidated.

Further, lipid biomarkers for weaning stress in jejunal crypt cells of early-weaned piglets were identified. The top 9 markers belonged to PE, PC, SM, PI, carnitine, and Hex2Cer classes. Reportedly, most of these markers are involved in different pathological progress. PC (9:0/26:1), SM (d14:1/22:0), and PC (17:0/18:2) are differentially expressed lipid species between early-stage non-small cell lung cancer and healthy control group

(Chen et al. 2018a, 2018b; Meng et al., 2021). The carnitine (24:0) level is significantly different between the myocardial infarction and control group (Lu et al., 2017). Moreover, PE (P-16:0/20:4) level is closely related to Alzheimer's Disease cognitive impairment and colorectal cancer (Bennett et al., 2013; Shu et al., 2018). Hence, lipid biomarkers in this study might participate in the pathological changes (such as inflammation) in the jejunal crypt cells after weaning. However, the exact function of these lipid species is poorly studied. To the best of our knowledge, this is the first time that lipid biomarkers for weaning stress in jejunal crypt cells have been explored.

5. Conclusion

In the current study, we found significant organ indexes, serum biochemical indexes, pro-inflammatory cytokine mRNA expression, lipid composition, and lipid metabolism pathway differences in jejunal crypt cells among piglets on different PWD, especially between PWD 3 and 14. Clear evidence showed that weaning stress led to remarkable changes in the jejunal crypt lipid profile, which might be related to the inflammation caused by weaning. Further, we found potential lipid biomarkers for weaning stress, which might be worthwhile therapeutic targets for weaning stress-induced intestinal diseases. However, their exact functions require further investigation.

Author contributions

Xia Xiong, **Yulong Yin**, and **Kexing Wang** designed the experiments; **Kexing Wang** and **Yirui Shao** conducted the experiments; **Jian Zhou** and **Lijun Zou** helped with animal experiments; **Yirui Shao** wrote the manuscript; **Xia Xiong**, **Pi Cheng**, **Lijun Zou**, and **Ming Qi** revised the manuscript. All authors have read and agreed to the published version of the manuscript.

Declaration of competing interest

We declare that we have no financial and personal relationships with other people or organizations that can inappropriately influence our work, and there is no professional or other personal interest of any nature or kind in any product, service and/or company that could be construed as influencing the content of this paper.

Acknowledgments

Appendix supplementary data

Supplementary data to this article can be found online at https://doi.org/10.1016/j.aninu.2022.07.001.

References

Andersson-Rolf A, Zilbauer M, Koo B-K, Clevers H. Stem cells in repair of gastrointestinal epithelia. Physiology 2017;32(4):278–89.

Barker N. Adult intestinal stem cells: critical drivers of epithelial homeostasis and regeneration. Nat Rev Mol Cell Biol 2014;15(1):19–33.

Bennett S, Valenzuela N, Xu H, Franko B, Fai S, Figeys D. Using neurolipidomics to identify phospholipid mediators of synaptic (dys)function in Alzheimer's Disease. Front Physiol 2013;4(168).

Braun A, Treede I, Gotthardt D, Tietje A, Zahn A, Ruhwald R, et al. Alterations of phospholipid concentration and species composition of the intestinal mucus barrier in ulcerative colitis: a clue to pathogenesis. Inflamm Bowel Dis 2009;15(11):1705–20.

Campbell JM, Crenshaw JD, Polo J. The biological stress of early weaned piglets. J Anim Sci Biotechnol 2013;4(1):19.

Castillo M, Martín-Orúe SM, Nofrarías M, Manzanilla EG, Gasa J. Changes in caecal microbiota and mucosal morphology of weaned pigs. Vet Microbiol 2007;124(3–4):239–47.

Chang B, Nishikawa M, Sato E, Utsumi K, Inoue M. l-Carnitine inhibits cisplatin-induced injury of the kidney and small intestine. Arch Biochem Biophys 2002;405(1):55–64.

Chen Y, Ma Z, Shen X, Li L, Zhong J, Min LS, et al. Serum lipidomics profiling to identify biomarkers for non-small cell lung cancer. BioMed Res Int 2018a;2018.

Chen Y, Ma Z, Zhong J, Li L, Min L, Xu L, et al. Simultaneous quantification of serum monounsaturated and polyunsaturated phosphatidylcholines as potential biomarkers for diagnosing non-small cell lung cancer. Sci Rep 2018b;8(1):1–13.

Cho E-j, Shin J-S, Noh Y-S, Cho Y-W, Hong S-J, Park J-H, et al. Anti-inflammatory effects of methanol extract of _Patrinia scabiosaefolia_ in mice with ulcerative colitis. J Ethnopharmacol 2011;136(3):428–35.

Constantin G, Laudanna C, Baron P, Berton G. Sulfatides trigger cytokine gene expression and secretion in human monocytes. FEBS Lett 1994;350(1):66–70.

Dong G, Pluske J. The low feed intake in newly-weaned pigs: problems and possible solutions. Asian Australas J Anim Sci 2007;20(3):440–52.

Espaillat MP, Kew RR, Obeid LM. Sphingolipids in neutrophil function and inflammatory responses: mechanisms and implications for intestinal immunity and inflammation in ulcerative colitis. Adv Biol Regul 2017;63:140–55.

Fabia R, Ar'Rajab A, Willén R, Andersson R, Ahrén B, Larsson K, et al. Effects of phosphatidylcholine and phosphatidylinositol on acetic-acid-induced colitis in the rat. Digestion 1992;53(1–2):35–44.

Gordon JI, Hermiston ML. Differentiation and self-renewal in the mouse gastrointestinal epithelium. Curr Opin Cell Biol 1994;6(6):795–803.

Hubler MJ, Kennedy AJ. Role of lipids in the metabolism and activation of immune cells. J Nutr Biochem 2016;34:1–7.

Ito K, Suda T. Metabolic requirements for the maintenance of self-renewing stem cells. Nat Rev Mol Cell Biol 2014;15(4):243–56.

Jeon S-B, Yoon HJ, Park S-H, Kim I-H, Park EJ. Sulfatide, a major lipid component of myelin sheath, activates inflammatory responses as an endogenous stimulator in brain-resident immune cells. J Immunol 2008;181(11):8077–87.

Khan MF, Wu X, Boor PJ, Ansari GA. Oxidative modification of lipids and proteins in aniline-induced splenic toxicity. Toxicol Sci 1999;48(1):134–40.

Latham NR, Mason G. Maternal deprivation and the development of stereotypic behaviour. Appl Anim Behav Sci 2008;110(1–2):84–108.

Lecce JG. Diarrhea: the nemesis of the artificially reared, early weaned piglet and a strategy for defense. J Anim Sci 1986;63(4):1307–13.

Li Q, Liang X, Xue X, Wang K, Wu L. Lipidomics provides novel insights into understanding the bee pollen lipids transepithelial transport and metabolism in human intestinal cells. J Agric Food Chem 2020;68(3):907–17.

Li R, Li L, Hong P, Lang W, Hui J, Yang Y, et al. β-Carotene prevents weaning-induced intestinal inflammation by modulating gut microbiota in piglets. Anim Biosci 2021;34(7):1221–34.

Li Z, Agellon LB, Allen TM, Umeda M, Jewell L, Mason A, et al. The ratio of phosphatidylcholine to phosphatidylethanolamine influences membrane integrity and steatohepatitis. Cell Metabol 2006;3(5):321–31.

Lin M, Weng S-Y, Chai K-F, Mao Z-J. Lipidomics as a tool of predicting progression from non-alcoholic fatty pancreas disease to type 2 diabetes mellitus. RSC Adv 2019;9(71):41419–30.

Livak KJ, Schmittgen TD. Analysis of relative gene expression data using real-time quantitative PCR and the 2−ΔΔCT method. Methods 2001;25(4):402–8.

Lu J, Chen B, Chen T, Guo S, Xue X, Chen Q, et al. Comprehensive metabolomics identified lipid peroxidation as a prominent feature in human plasma of patients with coronary heart diseases. Redox Biol 2017;12:899–907.

Martin TFJ. Phosphoinositide lipids as signaling molecules: common themes for signal transduction, cytoskeletal regulation, and membrane trafficking. Annu Rev Cell Dev Biol 1998;14(1):231–64.

Meng Q, Hu X, Zhao X, Kong X, Meng Y-M, Chen Y, et al. A circular network of coregulated sphingolipids dictates lung cancer growth and progression. EBioMedicine 2021;66:103301.

Meng Q, Sun S, Luo Z, Shi B, Shan A, Cheng B. Maternal dietary resveratrol alleviates weaning-associated diarrhea and intestinal inflammation in pig offspring by changing intestinal gene expression and microbiota. Food Funct 2019;10(9):5626–43.

NRC. Nutrient requirements of swine. National Academies Press; 2012.

Palm W, Rodenfels J. Understanding the role of lipids and lipoproteins in development. Development 2020;147(24):dev186411.

Qi M, Wang J, Tan Be, Li J, Liao S, Liu Y, et al. Dietary glutamine, glutamate, and aspartate supplementation improves hepatic lipid metabolism in post-weaning piglets. Anim Nutr 2020;6(2):124–9.

Ren W, Yan H, Yu B, Walsh MC, Yu J, Zheng P, et al. Prevotella-rich enterotype may benefit gut health in finishing pigs fed diet with a high amylose-to-amylopectin ratio. Anim Nutr 2021.

Shu X, Xiang YB, Rothman N, Yu D, Li HL, Yang G, et al. Prospective study of blood metabolites associated with colorectal cancer risk. Int J Cancer 2018;143(3):527–34.

Smith F, Clark JE, Overman BL, Tozel CC, Huang JH, Rivier JE, et al. Early weaning stress impairs development of mucosal barrier function in the porcine intestine. Am J Physiol Gastrointest Liver Physiol 2010;298(3):G352–63.

Su J, Zhang W, Ma C, Xie P, Blachier F, Kong X. Dietary supplementation with xylo-oligosaccharides modifies the intestinal epithelial morphology, barrier function and the fecal microbiota composition and activity in weaned piglets. Front Vet Sci 2021;8.

Suzuki T, Mochizuki K, Goda T. Localized expression of genes related to carbohydrate and lipid absorption along the crypt–villus axis of rat jejunum. Biochim Biophys Acta 2009;1790(12):1624–35.

van Beers-Schreurs HMG, Nabuurs MJA, Vellenga L, Valk HJK-vd, Wensing T, Breukink HJ. Weaning and the weanling diet influence the villous height and crypt depth in the small intestine of pigs and alter the concentrations of short-chain fatty acids in the large intestine and blood. J Nutr 1998;128(6):947–53.

van der Flier LG, Clevers H. Stem cells, self-renewal, and differentiation in the intestinal epithelium. Annu Rev Physiol 2009;71:241–60.

van der Veen JN, Kennelly JP, Wan S, Vance JE, Vance DE, Jacobs RL. The critical role of phosphatidylcholine and phosphatidylethanolamine metabolism in health and disease. Biochim Biophys Acta Biomembr 2017;1859(9 Pt B):1558–72.

Walther TC, Farese Jr RV. Lipid droplets and cellular lipid metabolism. Annu Rev Biochem 2012;81:687–714.

Wang B, Rong X, Palladino END, Wang J, Fogelman AM, Martín MG, et al. Phospholipid remodeling and cholesterol availability regulate intestinal stemness and tumorigenesis. Cell Stem Cell 2018a;22(2):206–220.e4.

Wang C, Cao S, Zhang Q, Shen Z, Feng J, Hong Q, et al. Dietary tributyrin attenuates intestinal inflammation, enhances mitochondrial function, and induces mitophagy in piglets challenged with diquat. J Agric Food Chem 2019;67(5):1409–17.

Wang L, Zhu C. Evidence from neonatal piglets shows how infant formula and other mammalian milk shape lipid metabolism. J Agric Food Chem 2021;69(6):1831–41.

Wang W, Zhao L, He Z, Wu N, Li Q, Qiu X, et al. Metabolomics-based evidence of the hypoglycemic effect of Ge-Gen-Jiao-Tai-Wan in type 2 diabetic rats via UHPLC-QTOF/MS analysis. J Ethnopharmacol 2018b;219:299–318.

Widowski TM, Torrey S, Bench CJ, Gonyou HW. Development of ingestive behaviour and the relationship to belly nosing in early-weaned piglets. Appl Anim Behav Sci 2008;110(1–2):109–27.

Xiong X, Yang H, Tan B, Yang C, Wu M, Liu G, et al. Differential expression of proteins involved in energy production along the crypt-villus axis in early-weaning pig small intestine. Am J Physiol Gastrointest Liver Physiol 2015;309(4):G229–37.

Yang F, Liu M, Qin N, Li S, Yu M, Wang C, et al. Lipidomics coupled with pathway analysis characterizes serum metabolic changes in response to potassium oxonate induced hyperuricemic rats. Lipids Health Dis 2019;18(1):112.

Yang H, Xiong X, Wang X, Li T, Yin Y. Effects of weaning on intestinal crypt epithelial cells in piglets. Sci Rep 2016;6:36939.

Yang H, Xiong X, Yin Y. Development and renewal of intestinal villi in pigs. In: Blachier F, Wu G, Yin Y, editors. Nutritional and physiological functions of amino acids in pigs. Vienna: Springer Vienna; 2013a. p. 29–47. https://doi.org/10.1007/978-3-7091-1328-8_3.

Yang HS, Fu DZ, Kong XF, Wang WC, Yang XJ, Nyachoti CM, et al. Dietary supplementation with N-carbamylglutamate increases the expression of intestinal amino acid transporters in weaned Huanjiang mini-pig piglets. J Anim Sci 2013b;91(6):2740–8.

Yin J, Li Y, Zhang X, Zeng X, Li T, et al. Long-term effects of lysine concentration on growth performance, intestinal microbiome, and metabolic profiles in a pig model. Food Funct 2018;9(8):4153–63.

Yin J, Wu MM, Xiao H, Ren WK, Duan JL, Yang G, et al. Development of an antioxidant system after early weaning in piglets. J Anim Sci 2014;92(2):612–9.

Yuan Y, Guo H, Zhang Y, Zhou D, Gan P, Liang DM, et al. Protective effects of L-carnitine on intestinal ischemia/reperfusion injury in a rat model. J Clin Med Res 2011;3(2):78–84.

Zhou Z, Zhang J, Zhang X, Mo S, Tan X, Wang L, et al. The production of short chain fatty acid and colonic development in weaning piglets. J Anim Physiol Anim Nutr 2019;103(5):1530–7.